

Supporting Information

Surfactant-assisted self-assembled polymorphs of AIE luminogen

di(4-propoxyphenyl) dibenzofulvene

Lufang Peng, Ya-Nan Chen, Yong Qiang Dong, Changcheng He* and Huiliang Wang*

Beijing Key Laboratory of Energy Conversion and Storage Materials, College of Chemistry,

Beijing Normal University, Beijing 100875, China.

E-mail: herbert@bnu.edu.cn (Changcheng He); wanghl@bnu.edu.cn (Huiliang Wang)

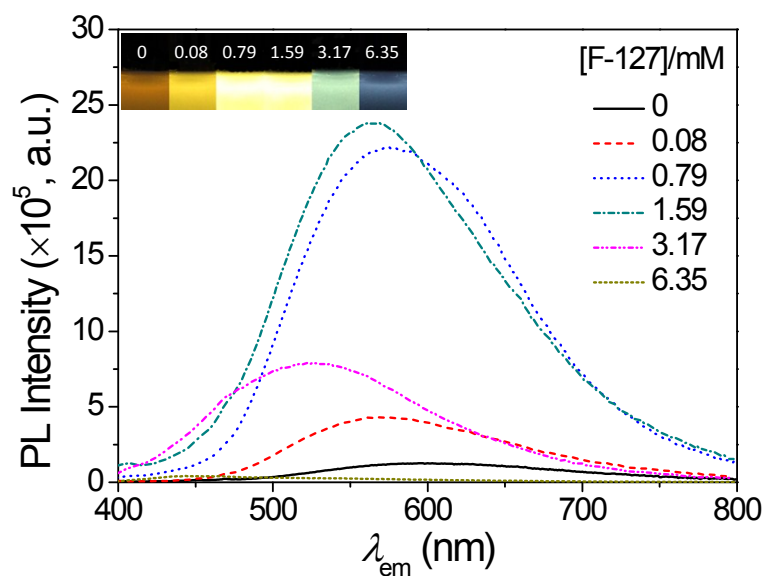


Fig. S1. PL spectra of the DBF dispersions with different F-127 concentrations. Inset: Photos of the DBF dispersions under UV illumination. $C_{\text{DBF}} = 1 \times 10^{-4} \text{ M}$, $f_w = 90\%$.

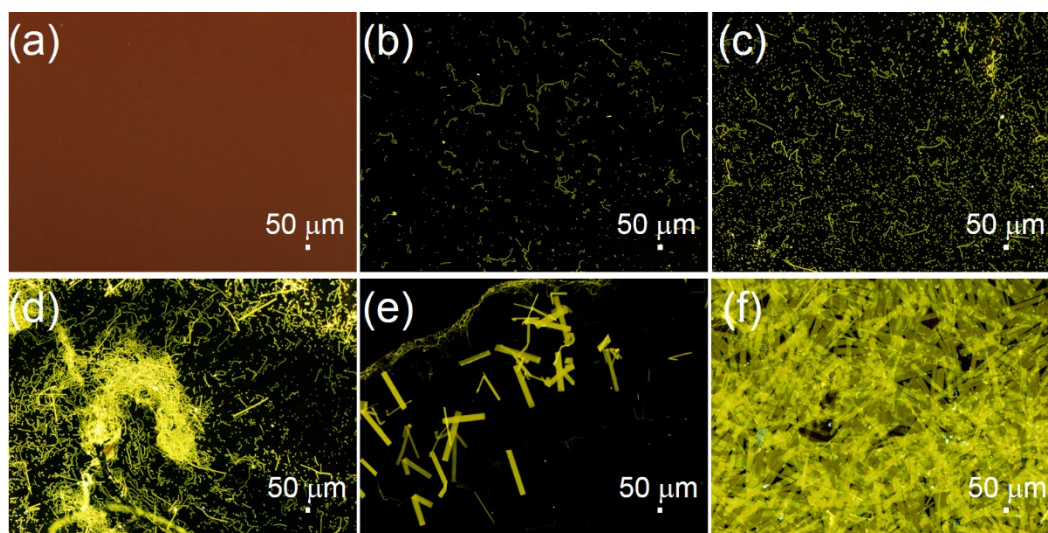


Fig. S2 Fluorescence microscopy images of the aggregates in the DBF dispersions with different SDBS concentrations. (a) 0 mM, (b) 0.5 mM, (c) 1.0 mM, (d) 1.2 mM, (e) 1.6 mM, and (f) 2.0 mM. $C_{\text{DBF}} = 1 \times 10^{-4} \text{ M}$, $f_w = 90\%$.

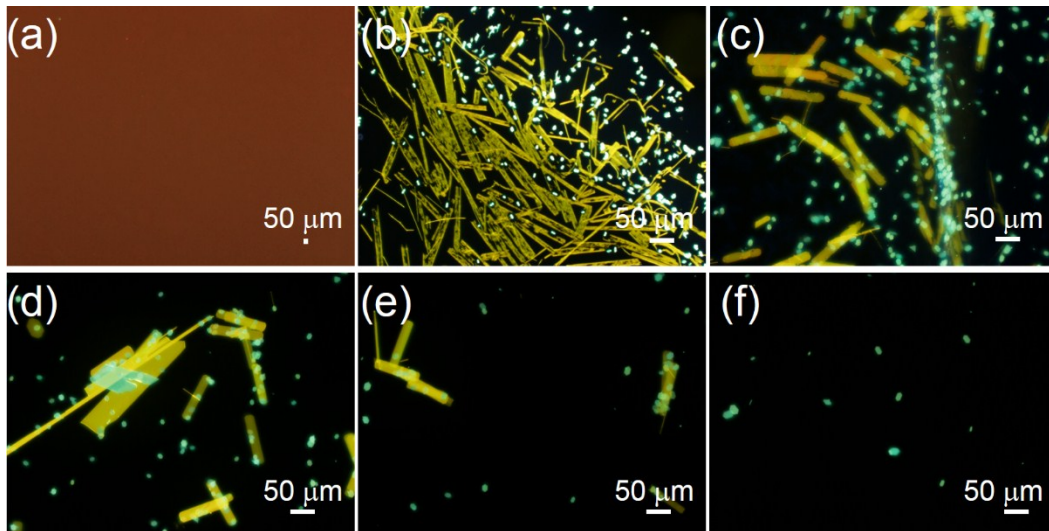


Fig. S3 Fluorescence microscopy images of the aggregates in the DBF dispersions with different F-127 concentrations. (a) 0 mM, (b) 0.08 mM, (c) 0.79 mM, (d) 1.59 mM, (e) 3.17 mM, and (f) 6.35 mM. $C_{\text{DBF}} = 1 \times 10^{-4}$ M, $f_w = 90\%$.

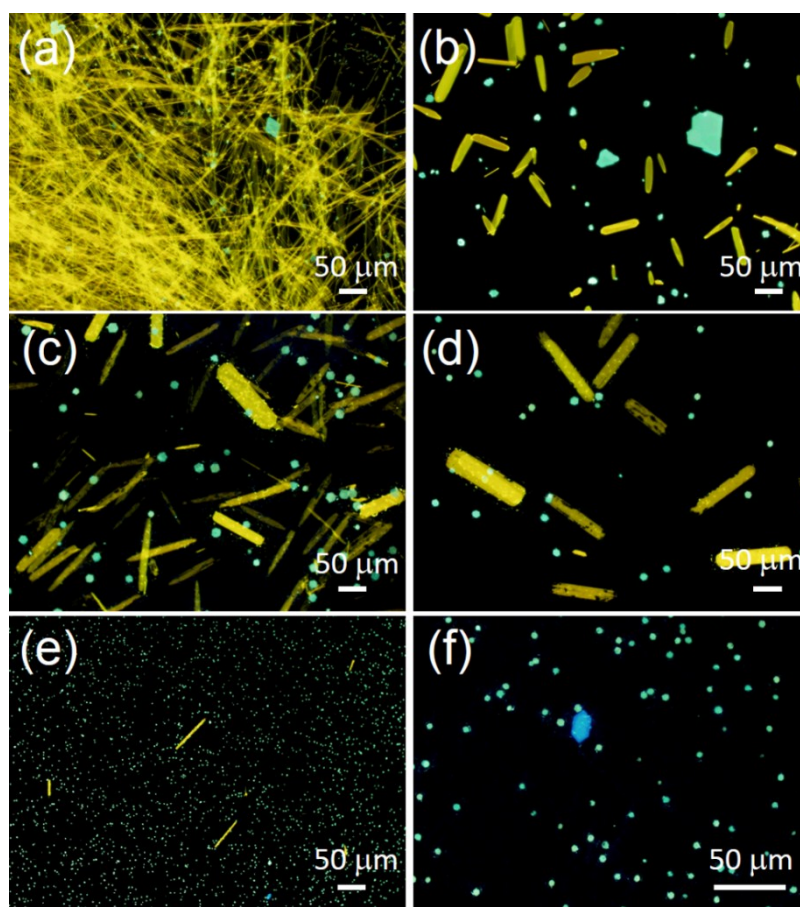


Fig. S4 Fluorescence microscopy images of the DBF dispersions with different molar ratios of SDBS to F-127. (a) SDBS/F-127 = 1.2 mM/0 mM, (b) SDBS/F-127 = 1.2 mM/0.6 mM, (c) SDBS/F-127 = 1.2 mM/1.2 mM, (d) SDBS/F-127 = 1.2 mM/1.8 mM, (e) SDBS/F-127 = 1.2 mM/2.4 mM, and (f) is the magnification of (e). $C_{\text{DBF}} = 1 \times 10^{-4}$ M, $f_w = 90\%$.

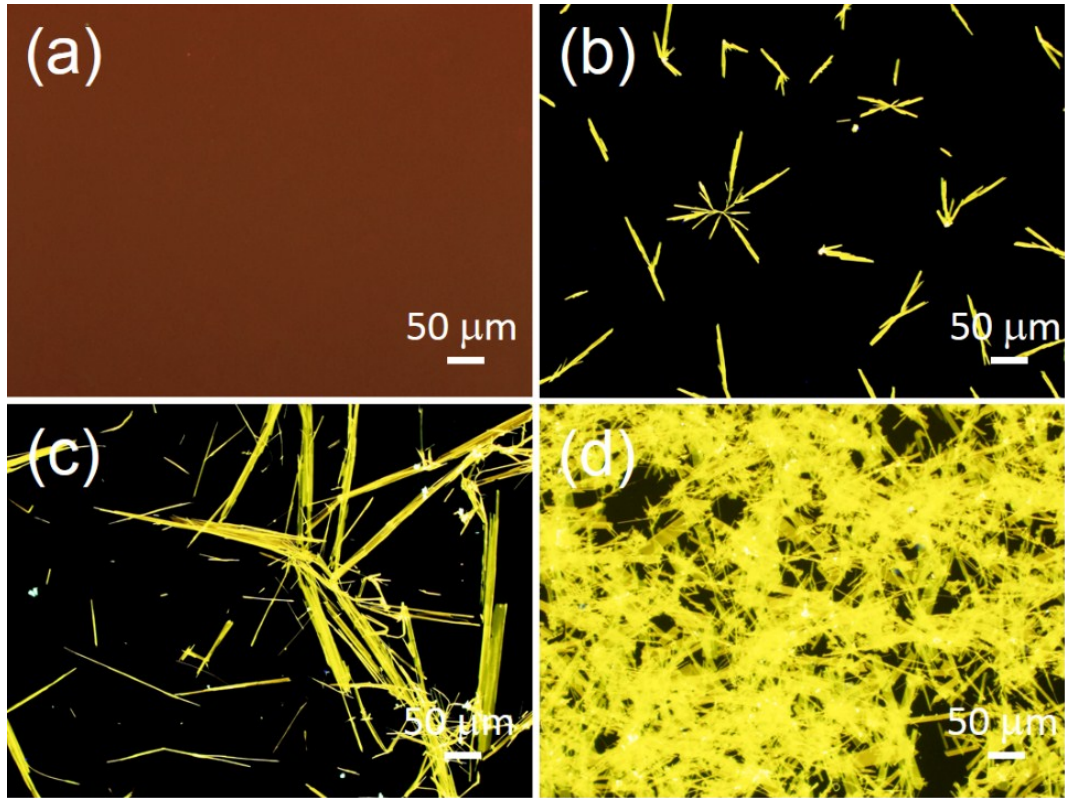


Fig. S5 Fluorescence microscopy images of the DBF dispersions kept at room temperature for different periods. (a)

0 d, (b) 3 d, (c) 5 d, and (d) 7 d. $C_{\text{DBF}} = 1 \times 10^{-4} \text{ M}$, $f_w = 90\%$, $C_{\text{SDBS}} = 2.0 \text{ mM}$.

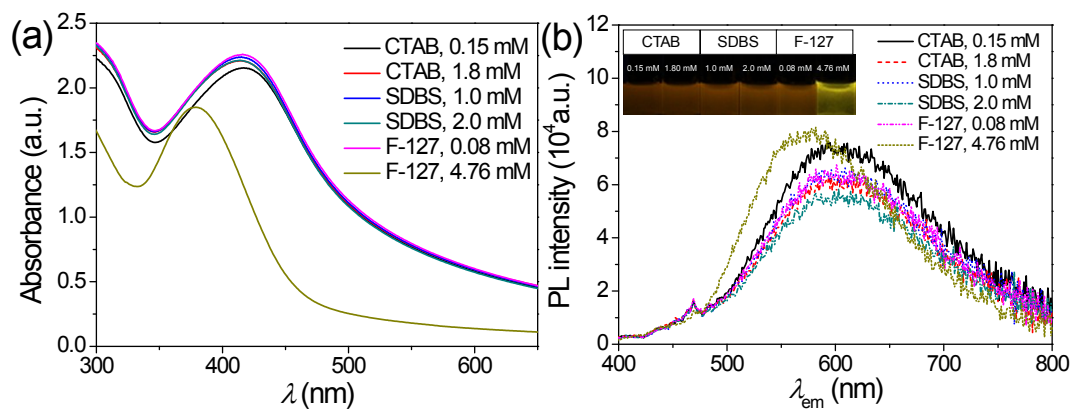


Fig. S6 (a) UV-visible and (b) PL spectra of the DBF dispersions with different surfactants. Inset in (b): Photos of the DBF dispersions under UV illumination. $C_{\text{DBF}} = 1 \times 10^{-4} \text{ M}$, $f_w = 90\%$. The dispersions were kept at 5°C for 7 d.

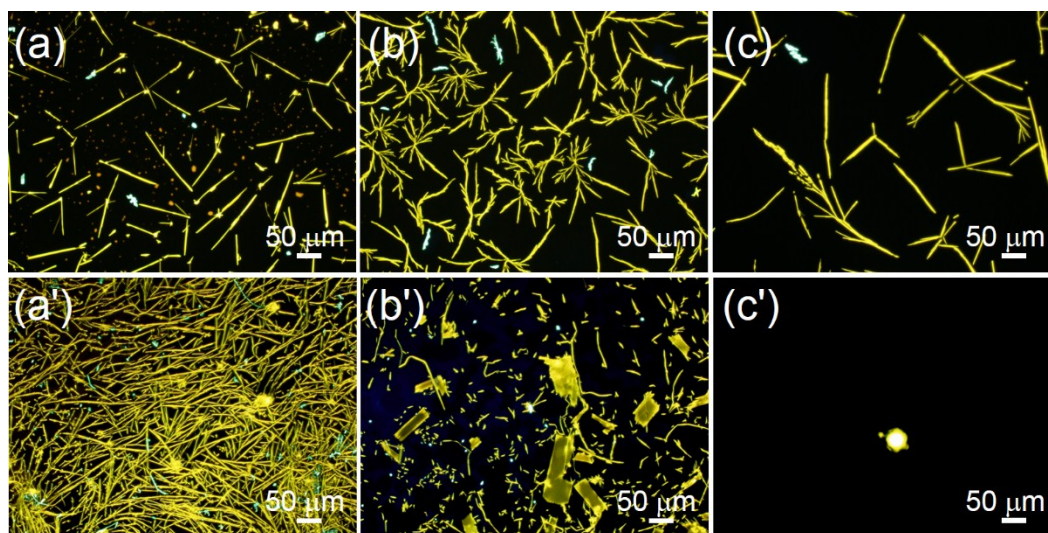


Fig. S7 Fluorescent microscopy images of the aggregates in the DBF dispersions with different surfactants. (a) 0.15 mM CTAB, (a') 1.8 mM CTAB, (b) 1.0 mM SDBS, (b') 2.0 mM SDBS, (c) 0.08 mM F-127, (c') 4.76 mM F-127. $C_{\text{DBF}} = 1 \times 10^{-4} \text{ M}$, $f_w = 90\%$. The dispersions were kept at 5°C for 7 d.

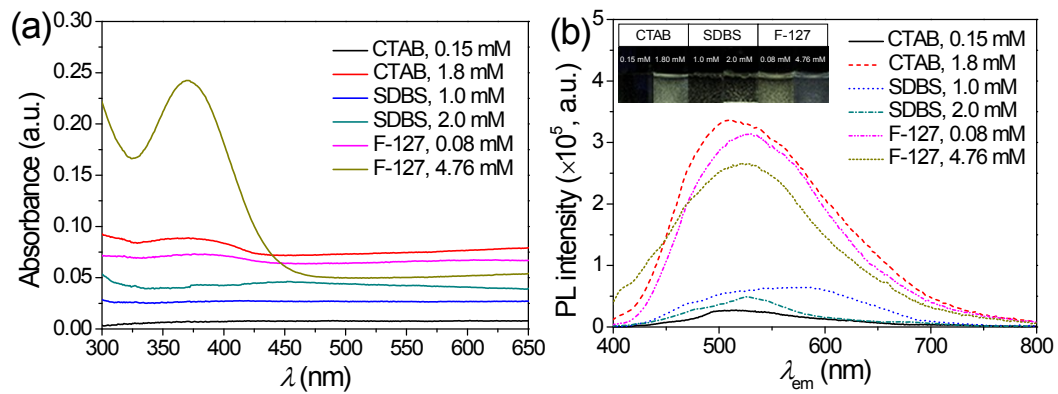


Fig. S8 (a) UV-visible and (b) PL spectra of the DBF dispersions with different surfactants. Inset in (b): Photos of the DBF dispersions under UV illumination. $C_{\text{DBF}} = 1 \times 10^{-4} \text{ M}$, $f_w = 90\%$. The dispersions were frozen at -20°C for 24 h before their storage for 7 d.

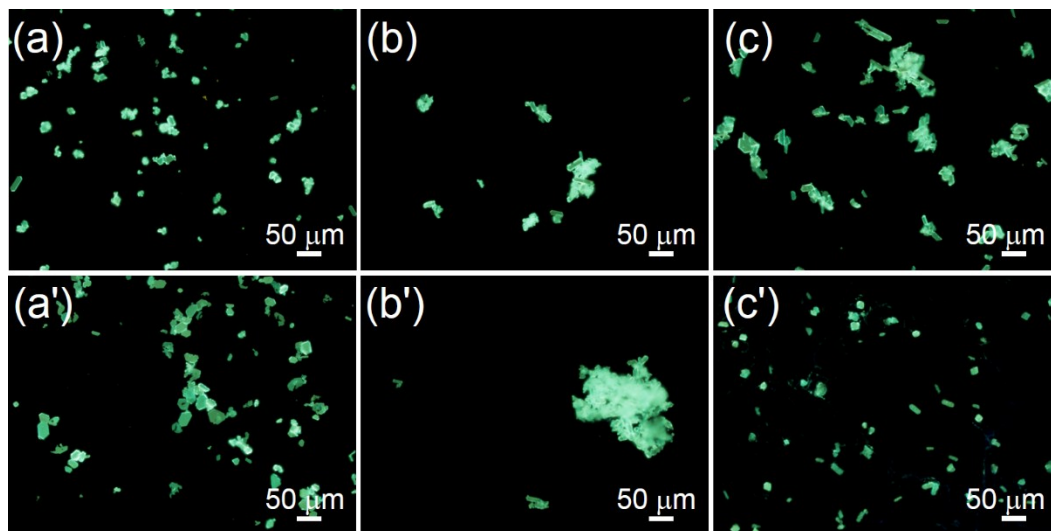


Fig. S9 Fluorescent microscopy images of the aggregates in the DBF dispersions with different surfactants. (a) 0.15 mM CTAB, (a') 1.8 mM CTAB, (b) 1.0 mM SDBS, (b') 2.0 mM SDBS, (c) 0.08 mM F-127, (c') 4.76 mM F-127. $C_{\text{DBF}} = 1 \times 10^{-4} \text{ M}$, $f_w = 90\%$. The dispersions were frozen at -20°C for 24 h before their storage for 7 d.

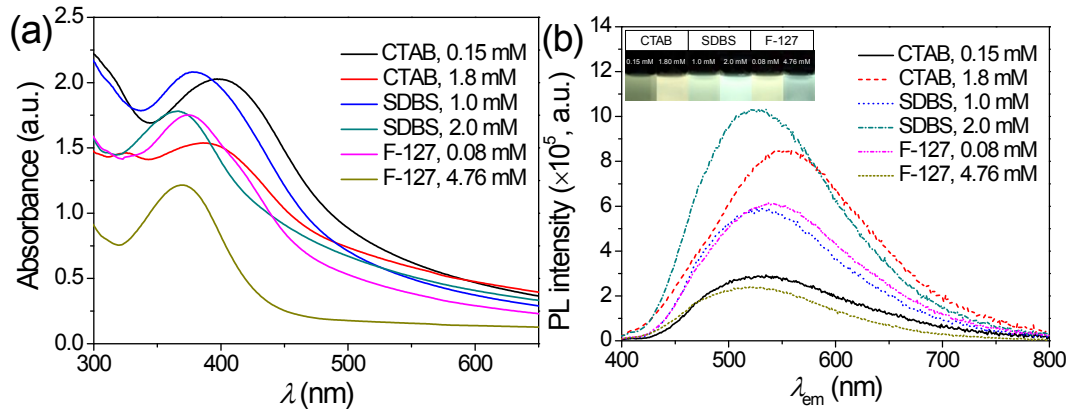


Fig. S10 (a) UV-visible and (b) PL spectra of the DBF dispersions with different surfactants. Inset in (b): Photos of the DBF dispersions under UV illumination. $C_{DBF} = 1 \times 10^{-4}$ M, $f_w = 90\%$. The dispersions were magnetically stirred for 15 h before their storage for 7 d.

Fig. S10 shows the UV-visible and PL spectra of the DBF dispersions with different surfactants after mechanical stirring. With comparison to the dispersions kept at R. T., the overall λ_{abs}^{max} have a significant blue-shift (Fig. S11a). When the surfactant concentrations are lower than their CMCs, the λ_{abs}^{max} are blue-shifted to 397 nm (CTAB), 377 nm (SDBS) and 375 nm (F-127), respectively. And the λ_{abs}^{max} are further blue-shifted to 386 nm (CTAB), 367 nm (SDBS) and 369 nm (F-127) when the concentrations of the surfactants are higher than their CMCs.

Their emission colours also have a corresponding blue-shift. For the DBF dispersions with CTAB, it has an abnormal red-shift from 531 nm (green light) to 551 nm (yellow-green light) when the CTAB concentration changes from low to high. And for the DBF dispersions with SDBS and F-127, they emit green colour ($\lambda_{em}^{max} = 531$ nm) and yellow-green colour ($\lambda_{em}^{max} = 541$ nm) at low concentrations, respectively, while at high concentrations are blue-shifted to green fluorescence ($\lambda_{em}^{max} \approx 522$ nm) with different luminous intensities.

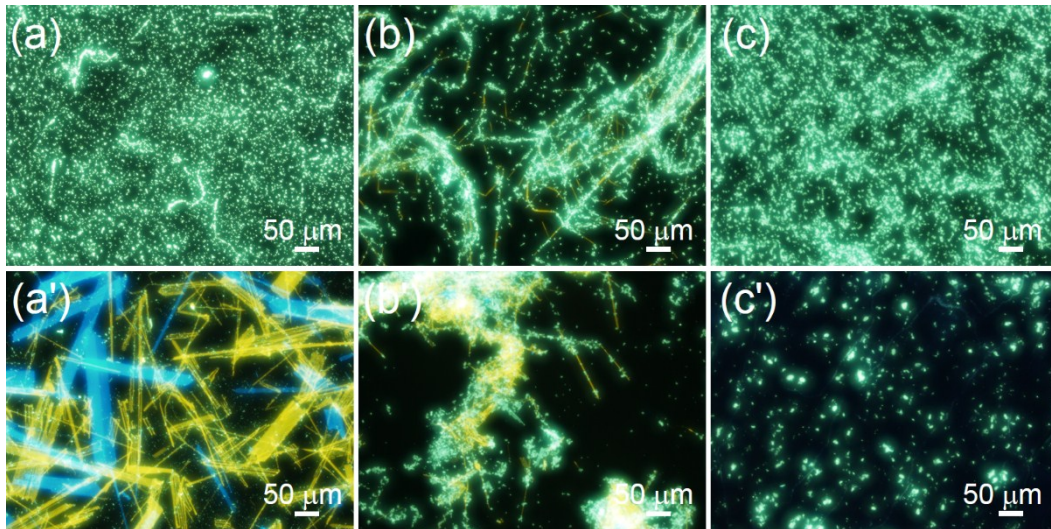


Fig. S11 Fluorescent microscopy images of the DBF aggregates in the dispersions with different surfactants. (a) 0.15 mM CTAB, (a') 1.8 mM CTAB, (b) 1.0 mM SDBS, (b') 2.0 mM SDBS, (c) 0.08 mM F-127, (c') 4.76 mM F-127. The dispersions were mechanically stirred for 15 h before their storage for 7 d. $C_{\text{DBF}} = 1 \times 10^{-4}$ M, $f_w = 90\%$.

Green-emitting particles are found in all dispersions that are stirred. In addition to green particles, there are many yellow- and blue-emitting sheets in the dispersion with a high concentration of CTAB, along with yellow- and blue-emitting needles (Fig. S11a'). And for the dispersions with SDBS, filaments with yellow emission are observed at a low concentration, while yellow-emitting needles and blue-emitting sheets are found at a high concentration (Fig. S11b, b'). Only green hexagonal structures were obtained in the dispersions with F-127 whatever the concentration is lower or higher than its CMC (Fig. S11c, c').

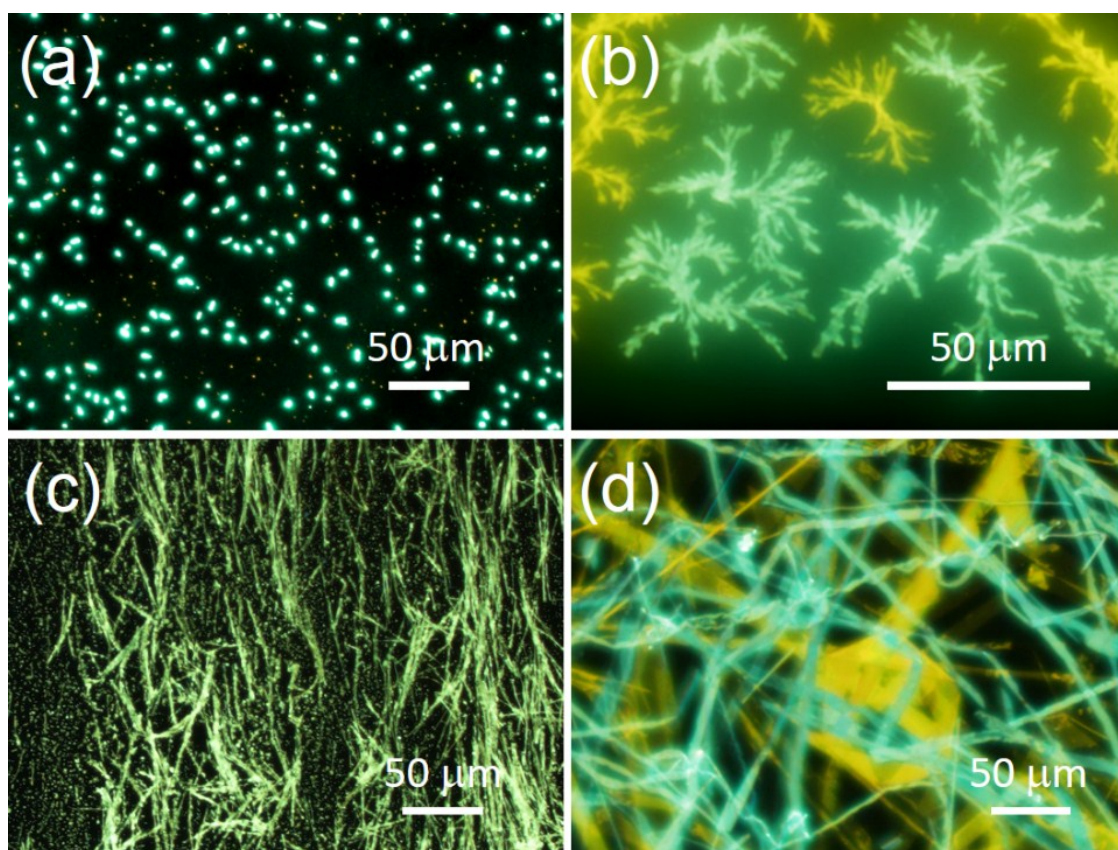


Fig. S12 Fluorescent microscopy images of the green-emitting aggregates in the forms of (a) particles, (b) dendritic structures, (c) needles and (d) ribbons formed in the dispersions with different concentrations of CTAB under different conditions. (a) 0.15 mM after mechanical stirring, (b) 0.15 mM at R. T., (c) 1.0 mM after mechanical stirring, and (d) 1.0 mM at R. T. $C_{\text{DBF}} = 1 \times 10^{-4} \text{ M}$, $f_w = 90\%$.

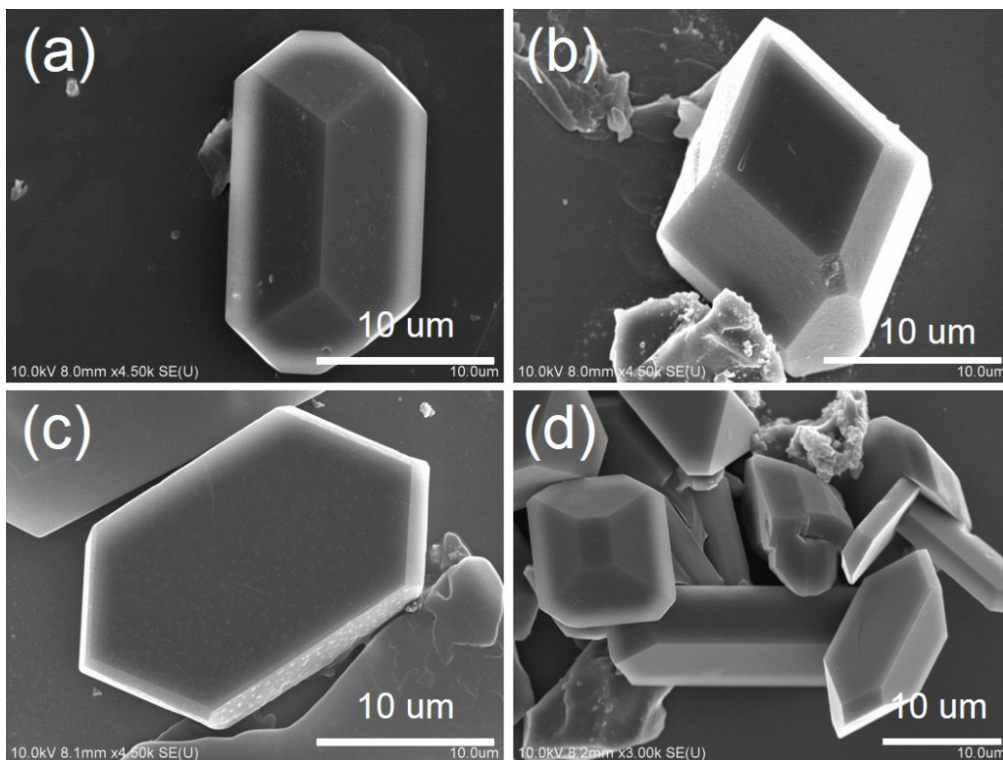


Fig. S13 SEM images of the hexagonal and rhombic particles with various morphologies. $C_{\text{DBF}} = 1 \times 10^{-4} \text{ M}$, $f_w = 90\%$.

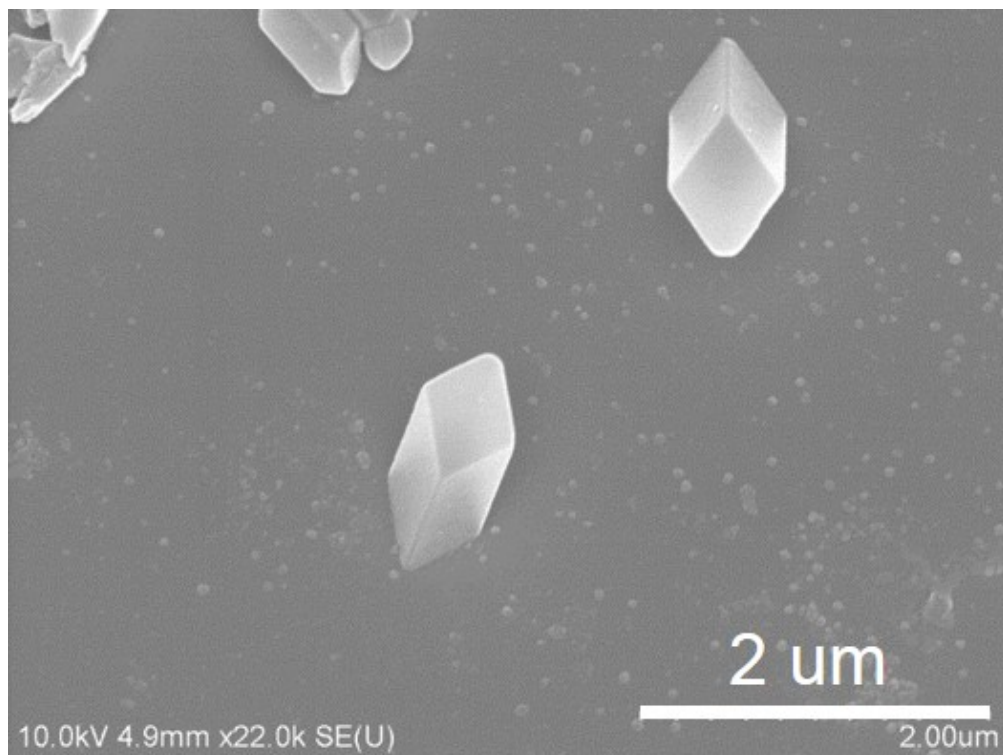


Fig. S14 SEM image of the rhombic 3D structure. SDBS/CTAB = 1.2 mM/2.4 mM, $C_{\text{DBF}} = 1 \times 10^{-4} \text{ M}$, $f_w = 90\%$.

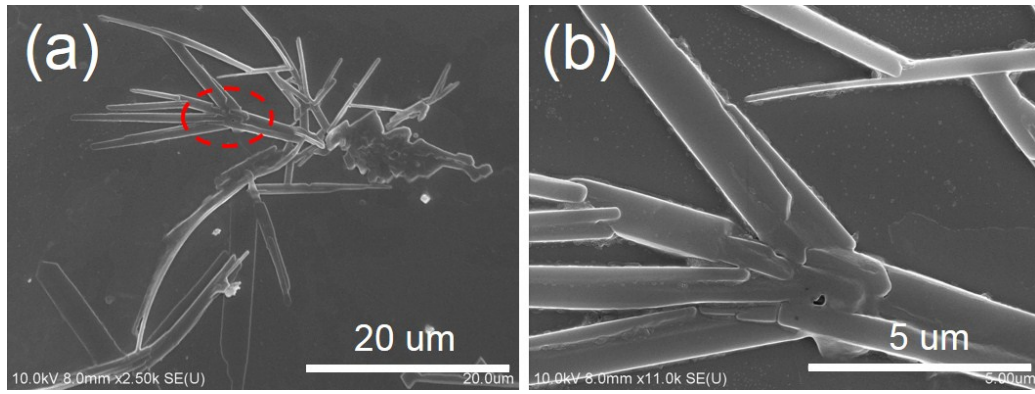


Fig. S15 (a) SEM images of the dendritic structure and (b) the magnification of the red circle. $C_{\text{DBF}} = 1 \times 10^{-4} \text{ M}$, $f_w = 90\%$.

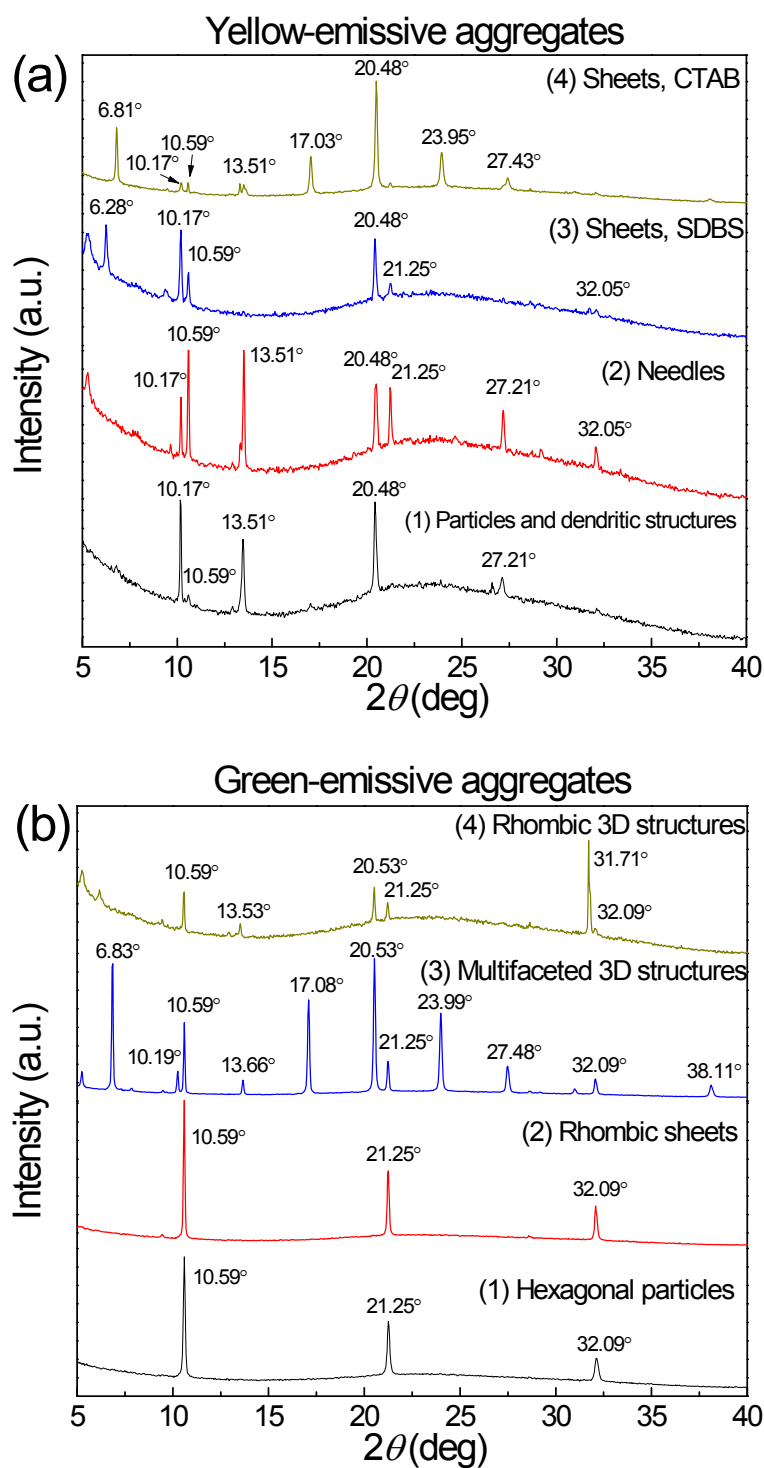


Fig. S16 (a) XRD patterns of the yellow-emitting aggregates: (1) particles and dendritic structures: 0.15 mM CTAB at R. T., (2) needles: 1.0 mM SDBS at 5°C, (3) sheets: 2.0 mM SDBS at R. T., (4) sheets: 1.8 mM CTAB at R. T. (b) XRD patterns of the green-emitting aggregates: (1) hexagonal particles: 0.08 mM F-127 after mechanical stirring, (2) rhombic sheets: SDBS/CTAB = 1.2 mM/4.8 mM at R. T., (3) multifaceted 3D structures: 2.0 mM SDBS after FT treatment, (4) rhombic 3D structures: SDBS/CTAB = 1.2 mM/4.8 mM after FT treatment. $C_{\text{DBF}} = 1 \times 10^{-4}$ M, $f_w = 90\%$.

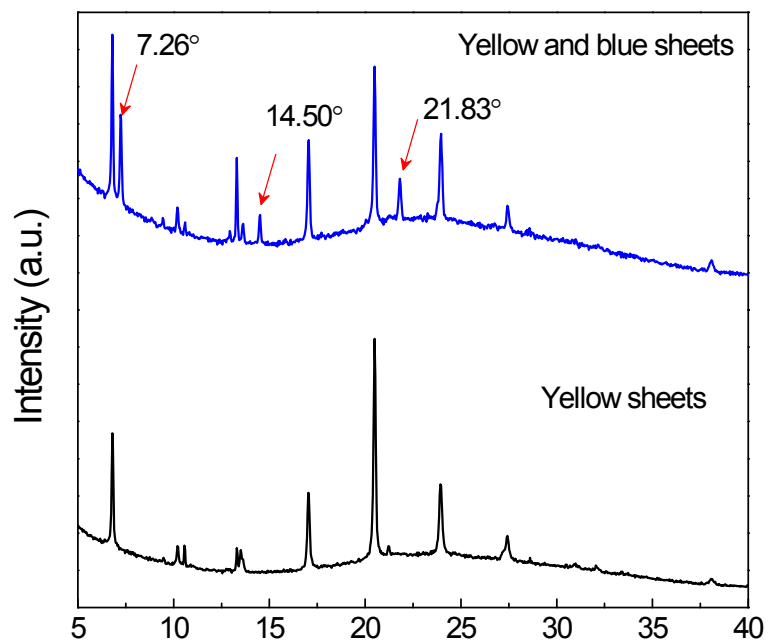


Fig. S17 XRD patterns of the yellow-emitting sheets (1.8 mM CTAB at R. T.), and yellow- and blue-emitting sheets (1.8 mM CTAB after mechanical stirring).